Colloid Polym Sci (2015) 293:165–176
DOI 10.1007/s00396-014-3405-7

ORIGINAL CONTRIBUTION

What makes AOT reverse micelles spherical?

Sergey A. Tovstun · Vladimir F. Razumov

Received: 9 June 2014 / Revised: 23 August 2014 / Accepted: 23 September 2014 / Published online: 1 October 2014

Abstract It is known that sodium bis(2-ethylhexyl) sulfosuccinate (AOT) reverse micelles are spherical over a wide range of water-to-surfactant molar ratios. This contradicts the traditional concept of preferred curvature. In actual fact, this concept does not apply to the AOT monolayer because its free energy is almost a linear function of the mean curvature. To correctly predict the shape of AOT reverse micelles, it is necessary to take into account not only the curvature free energy but also the disjoining pressure arising primarily from the overlapping of the electrical double layers at the opposite sides of the water core. Based on these considerations, we develop a model to calculate the free energy of AOT reverse microemulsion. This model allows us to explain the sphericity and to calculate various thermodynamic properties: the enthalpy of solubilization, chemical potentials, polydispersity, and the phase diagrams. All results are in qualitative agreement with the available experimental data.

Keywords Reverse micelles · Poisson–Boltzmann equation · Helfrich equation · Aerosol OT · Free energy · Disjoining pressure

Electronic supplementary material The online version of this article (doi:10.1007/s00396-014-3405-7) contains supplementary material, which is available to authorized users.

S. A. Tovstun (✉) · V. F. Razumov
Institute of Problems of Chemical Physics, Russian Academy of Sciences, Acad. Semenov av. 1, Chernogolovka, Moscow region 142432, Russia
e-mail: tovstun@icp.ac.ru

V. F. Razumov
e-mail: razumov@icp.ac.ru

Introduction

Reverse microemulsions are thermodynamically stable liquids whose structure may be viewed as an oil dispersion of reverse micelles (nanosized water droplets covered with a surfactant monolayer).

In reverse microemulsions, a portion of the surfactant is dissolved in the nonpolar intermicellar medium as individual molecules or their small aggregates. This fraction is negligibly small for ionic surfactants and large for nonionic surfactants [1]. Hereinafter, all surfactant is assumed to be situated at the oil–water interface.

The surfactant monolayer at the oil–water interface is closely packed because of the compressive action of the interfacial tension. Therefore, the area per surfactant molecule at the interface is nearly independent of the composition of reverse microemulsion. So, the amount of surfactant uniquely determines the area of the oil–water interface. The volume of the space enclosed by this interface is equal to the total volume of the water in the microemulsion.

Given the restrictions on the total enclosed volume and area of the interface, an uncountable set of its spatial configurations are hypothetically possible. Moreover, a portion of the water may form a separate phase. But, in reality, only the configuration with the lowest free energy may form spontaneously. Hence, the key question in understanding the structure of reverse microemulsions is as follows: how and why the free energy of the oil/water/surfactant system depends on the shape of the surfactant monolayer?

Traditionally, this question is addressed by using the concept of the curvature dependence of the free energy per unit area of the surface [2–6]. Local properties of any smooth surface at any point may be described by two parameters called principal curvatures c_1 and c_2. We take the curvature

to be positive for reverse micelles (traditionally, the opposite convention is used). The free energy per unit area of the surface σ may be expanded in powers of c_1 and c_2 up to the second order around the flat surface, for which $c_1=c_2=0$:

$$\sigma(c_1,c_2)=\sigma(0,0)+\frac{\partial\sigma(0,0)}{\partial c_1}c_1+\frac{\partial\sigma(0,0)}{\partial c_2}c_2+ +\frac{1}{2}\frac{\partial^2\sigma(0,0)}{\partial c_1^2}c_1^2+\frac{1}{2}\frac{\partial^2\sigma(0,0)}{\partial c_2^2}c_2^2+\frac{\partial^2\sigma(0,0)}{\partial c_1\partial c_2}c_1c_2. \quad (1)$$

In Eq. (1), under the assumption of no preferred direction on the surface, the symmetry allows us to equate the coefficients of curvatures c_1 and c_2 and also of their squares. With this assumption, we can rename the coefficients and rewrite Eq. (1) as

$$\sigma=\sigma_0+\frac{\kappa}{2}(c_1+c_2-2c_0)^2+\overline{\kappa}c_1c_2 \quad (2)$$

Equation (2) was originally derived by Helfrich [7] and since then has been used in many works to calculate the polydispersity and shape fluctuations of reverse micelles [8–17]. The constants κ and $\overline{\kappa}$ are called, respectively, the rigidity and the Gaussian rigidity of the surface. $c_0=1/r_S$ is the so-called spontaneous curvature, r_S is the so-called radius of spontaneous curvature. $\sigma_0=\sigma(0,0)-2\kappa c_0^2$ is just a constant.

The term "spontaneous curvature" for c_0 is somewhat misleading because if the minimum of the Helfrich free energy (2) exists (i.e., if $-2\kappa<\overline{\kappa}<0$), then it occurs at

$$c_1=c_2=\frac{c_0}{1+\overline{\kappa}/(2\kappa)} \quad (3)$$

but not at $c_1=c_2=c_0$ (see refs. [18, 19] or Online Resource). We will refer to (3) as the "optimal curvature." Moreover, since Eq. (2) is derived from the Taylor expansion, it is valid only for low curvatures (much less than the inverse thickness of the surface). But, for an arbitrary physical surface, the formally calculated optimal curvature (3) is not necessarily low and may lie outside the range of acceptable numerical accuracy of the expansion. In this case, it may not be regarded as a "true" optimal curvature. For example, for a symmetric (or nearly symmetric) lipid bilayer, the optimal curvature is low and may be calculated from Eq. (3). But, if we formally use the Helfrich equation for the calculation of the radius of the optimal curvature of the ionic surfactant monolayer, taking into account only the free energy of the electrical double layer, then we obtain an absurdly small value of the order of the Debye screening length at the surface (a few angstroms) [20–22]. But, in fact, such a surface does not have any optimal curvature at all, and its free energy is a monotonic function of the mean curvature.

When Eq. (2) is applied not to an imaginary infinitely thin mathematical surface but to a curved surfactant monolayer of a finite thickness, the problem arises that within the monolayer, the surface may be defined in a variety of ways. This difficulty can be overcome by taking into account that the use of Eq. (2) implies that the area per surfactant molecule is constant. Hence, Eq. (2) must be applied to the so-called surface of inextension [18, 23]. This surface is defined by the condition that the area of the cross-section of a surfactant molecule at this surface does not vary with small variations of the principal curvatures. The position of the surface of inextension may be dependent on the principal curvatures [23]. Roughly, it can be imagined that the surface of inextension passes through the thickest parts of the surfactant molecules.

The description of microemulsions by means of the Helfrich equation relies heavily on the concept of the optimal curvature of the surfactant monolayer. The optimal curvature must be sufficiently small so that large microemulsion droplets may be formed. Depending on the sign of the optimal curvature, a direct (oil in water) or a reverse microemulsion may be formed. The surfactant monolayer tends to adopt a conformation with principal curvatures that are closest to the optimal curvature while satisfying the constraints on the total amounts of water and surfactant available in the system. The tendency of the surfactant monolayer to make its principal curvatures close to the optimal curvature is a driving force for the solubilization of the dispersed phase.

For example, if we restrict our consideration of reverse microemulsions to the case of only spherical reverse micelles, assuming that other shapes are impossible, then we get the following picture. For a reverse microemulsion with small reverse micelles, the curvature of the surfactant monolayer is high. If such a microemulsion comes in contact with the water phase, then the tendency of the surfactant monolayer to adopt the optimal curvature will cause the solubilization of water until either the water phase disappears or until the principal curvatures become equal to the optimal curvature. In the last case, a two-phase system of the type "reverse microemulsion+water" is formed. Such an interpretation of the process of solubilization can be found, for example, in the papers [10–12, 17].

However, it is incorrect to arbitrarily restrict the consideration only to spherical reverse micelles, since, in principle, within the framework of the Helfrich equation, other shapes may have lower free energy. To show this, we have calculated the phase diagram of the reverse microemulsion system by minimizing its Helfrich free energy (2) for all water contents and ratios $\bar{\kappa}/\kappa$ (Fig. 1). Among the possible shapes of reverse micelles, we considered the sphere, the cylinder, and the lamella (flat bilayer). Common tangent construction was used to determine the coexistence of different shapes. The radius of

reverse micelles was related to the water-to-surfactant molar ratio W=[water]/[surfactant] by the equation

$$r_0 = \frac{nv}{a_0} W, \tag{4}$$

where n=1, 2, and 3 for, respectively, lamellar, cylindrical, and spherical reverse micelles, v is the volume of one water molecule (30 Å^3), and a_0 is the area per one surfactant molecule at the oil–water interface (for lamellar reverse micelles, the radius is defined as their half-thickness). The calculated phase diagram shows that spherical reverse micelles are stable only in a narrow range of water contents. At the lower left corner of the phase diagram, there is a broad region of coexistence of spherical or cylindrical reverse micelles with "dry" lamellar reverse micelles (the term "dry" means r_0=0). Lamellar reverse micelles arise because their principal curvatures at low water contents are closer to the optimal curvature than the principal curvatures of spherical or cylindrical reverse micelles. They turn out to be "dry" because it is more favorable to use the available water for the formation of spherical or cylindrical reverse micelles with principal curvatures close to the optimal curvature.

It follows from the calculated phase diagram that spherical reverse micelles are stable only in a relatively narrow range where the curvature of the surfactant monolayer is close to the optimal curvature. At the same time, for "classical" reverse microemulsions of sodium bis(2-ethylhexyl) sulfosuccinate (AOT), the stability region is quite large: under proper conditions, it can range from W=0 to about W=60. Hence, we must conclude that the AOT monolayer has no optimal curvature. In the context of Eqs. (1) and (2), this means that the second-order terms are much smaller than the first-order terms and therefore can be neglected. But, in this case, there would be no solubilization. The most obvious effect that can be taken into account to resolve this contradiction is the disjoining pressure in the microemulsion droplets. For reverse microemulsions of ionic surfactants with monovalent counterion, this disjoining pressure is positive and arises from the overlap of the electrical double layers (EDLs) formed at the opposite sides of the water core of the reverse micelle as a result of the dissociation of the surfactant molecules. The result of this overlap depends mainly on the size of the reverse micelle. This implies, in particular, that the free energy of the lamellar reverse micelle must depend on its thickness. Note that this does not obey the Helfrich equation. That the Helfrich equation fails to describe the overlap of the EDLs in the absence of added electrolyte is known in the literature [23, 24]. Thus, the free energy of reverse microemulsion must be determined not only by the surface integral of a certain function of the principal curvatures but also, somehow, by the distance between the oppositely located parts of the interface. We will refer to these contributions as the "surface contribution" and the "volume contribution," respectively. By considering the surface and volume contributions simultaneously, it is possible to consistently describe the dependence of the free energy of reverse microemulsion on the shape of the interface. Briefly, the volume contribution determines the tendency of reverse micelles to grow infinitely through the solubilization of water, while the surface contribution determines the most favorable shape.

In this paper, we present detailed calculations of the free energy of AOT reverse microemulsions, taking into account the surface and volume contributions. The calculations are performed as follows. We start by calculating the free energy of the EDL for spherical, cylindrical, and lamellar reverse micelles. The EDL provides us with the volume contribution to the free energy of a reverse micelle. For the sake of clarity, the calculations are performed analytically as far as possible, using a simplified model of the reverse micelle. Then, we qualitatively discuss what kind of surface contribution should be added to the EDL free energy in order to provide the thermodynamic stability of the spherical shape (AOT reverse micelles are usually spherical). Then, we develop a more accurate model of reverse micelle. Further calculations are carried out numerically.

The free energy of the EDL in reverse micelles of different shapes

Historical background

The dependence of the EDL free energy on the shape of the surfactant monolayer has been extensively studied at the end of the last century by several groups of theoreticians. Early studies [e.g., [20, 21, 25, 26]] were devoted to the case of high added salt concentration, when the long-range electrostatic interactions are screened and the EDL free energy of the whole surface is a sum of the free energies of its small parts. This case may be considered to be fully investigated. The results of the calculations were presented in terms of the coefficients of the Helfrich equation.

Subsequent studies [e.g., [22, 27–29]] were devoted to the case of low or zero added salt concentration. In this case, the long-range electrostatic interactions are not screened. Therefore, the local approximation does not work in its pure form: the dependence of the EDL free energy on the shape of the surfactant monolayer must be a certain complicated functional that takes into account the contributions from both the curvature and the disjoining pressure.

However, if we restrict ourselves to surfactant monolayer geometries with fixed thickness of the water region, then the disjoining pressure is also fixed and we can expect that the

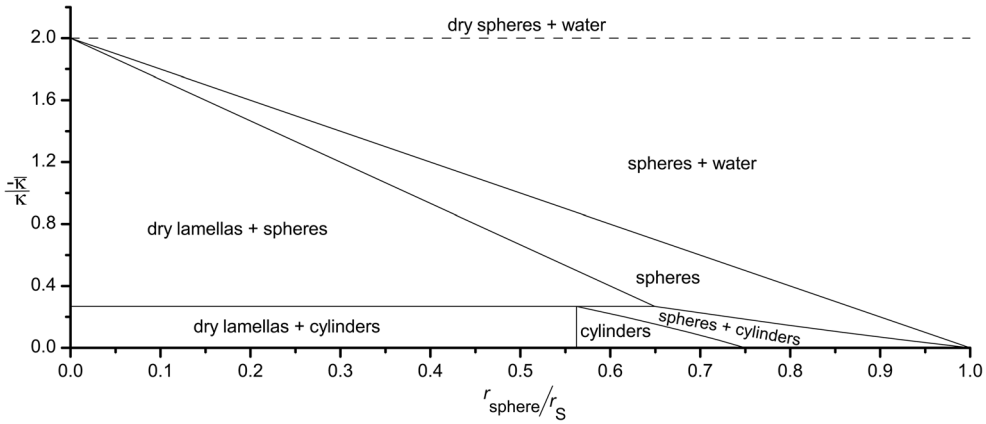

Fig. 1 Phase diagram of reverse microemulsion according to the Helfrich equation (2). The water content is expressed as a ratio r_{sphere}/r_S, where r_{sphere} is the radius of spherical reverse micelles that corresponds to a hypothetical situation in which there are only spherical reverse micelles, and they solubilized all the water. $\bar{\kappa} < 0 < \kappa$

EDL free energy depends only on the curvature. It is this kind of geometries that are considered in the studies [27–29, 22]: the EDL between two nearly flat monolayers undulating in-phase and the EDL between two concentric cylinders (or spheres) of large radii. Calculations on these geometries have led to the conclusion that the dependence of the EDL free energy on the shape of the surfactant monolayer may be described by the Helfrich equation and that the only effect of nonlocality of electrostatic interactions is that the coefficients in the Helfrich equation depend on the distance between the opposite monolayers. We note that some of these studies [27, 29] also considered the case of the EDL between two nearly flat monolayers undulating in antiphase, when the distance between the monolayers is not fixed but varies sinusoidally in one direction. In this case, the disjoining pressure must be taken into account, and an attempt to rely solely on the Helfrich equation leads to erroneous results.

Thus, the existing studies on the dependence of the EDL free energy on the shape of the surfactant monolayer extensively consider the curvature contribution but do not consider the contribution from the disjoining pressure. At the same time, for the purposes of the present study, it is necessary to know how the disjoining pressure depends on the shape of reverse micelles (sphere, cylinder, and lamella) and whether the decomposition of the free energy into the surface and volume contributions is indeed possible. All the EDL geometries considered in the existing literature (undulating monolayers and concentric cylinders or spheres of large radii) can be viewed as small deformations of the lamellar reverse micelle. But, we are interested in other shapes (sphere and cylinder). Therefore, we proceed by calculating the EDL free energies for the shapes of interest and then ascertaining whether the decomposition is possible.

Basic equations

We assume that the surfactant is completely dissociated and that the charges on the dissociated surfactant molecules are uniformly distributed on the surface of the water core. The electric field potential φ obeys the Poisson–Boltzmann equation (in SI units)

$$\Delta\varphi = \frac{-qc_0}{\varepsilon\varepsilon_0}\exp\left(-\frac{q\varphi}{kT}\right), \tag{5}$$

where ε is the dielectric constant of water, ε_0 is the electric constant, c_0 is the counterion concentration at the point where $\varphi=0$, k is the Boltzmann constant, T is the absolute temperature, and q is the counterion charge (note that the Poisson–Boltzmann equation is accurate enough only for monovalent counterions [30–32]). The boundary conditions for this equation are

$$\left.\frac{\partial\varphi}{\partial r}\right|_{r=r_0} = \frac{-q}{a_0\varepsilon\varepsilon_0}, \tag{6}$$

$$\left.\frac{\partial\varphi}{\partial r}\right|_{r=0} = 0, \tag{7}$$

$$\varphi(0) = 0, \tag{8}$$

where r is the distance from the center of the reverse micelle. Equation (6) follows the Gauss's law. Equation (7) is due to the symmetry. Equation (8) defines the point of zero potential (so, c_0 is the counterion concentration at the center of the reverse micelle). The radius of reverse micelles r_0 is defined by Eq. (4).

The free energy of the EDL is a sum $G_{EDL}=G_{el}+G_{mix}$ of the free energy of the electric field

$$G_{el} = \frac{\varepsilon\varepsilon_0}{2}\int(\nabla\varphi)^2 dV \tag{9}$$

and the free energy arising from the mixing of the counterions with water and from the spatial nonuniformity of the counterion distribution

$$G_{mix} = kT\int c\ln\frac{c}{ec_{ref}}dV, \tag{10}$$

where c_{ref} is the reference concentration at which the counterion chemical potential is assumed to be zero, e is the base of the natural logarithm, and c is the counterion concentration, which depends on r; the integration is performed over the volume V of the water core of the reverse micelle.

Solutions of the Poisson–Boltzmann equation

Solutions of the Poisson–Boltzmann equation (5) are obtained in Online Resource. Here, we only present the necessary results for the dependencies of the free energies on the water-to-surfactant molar ratio. Note that for the cases of lamellar and cylindrical reverse micelles, the solutions are known [33, 34], but we rederived them in order to have consistent free-energy expressions that can be compared to each other. To simplify further equations, we must define

$$W_0 = \left(2kTa_0^2\varepsilon\varepsilon_0\right)\Big/\left(q^2v\right) \tag{11}$$

and $\tilde{W}=W/W_0$. For AOT reverse micelles, Eq. (11) gives $W_0=3$.

The result for the free energy of the lamellar reverse micelle is

$$G_{EDL}^{lamella} = kTN_{surf}\left(-\ln\left(vc_{ref}e^2W_0\right)-2\ln\sin y_0 + y_0\cot y_0\right), \tag{12}$$

where N_{surf} is the number surfactant molecules in the reverse micelle, y_0 is a solution of the equation y_0 tan $y_0=\tilde{W}$. By using the asymptotic solutions of this equation, we can obtain the asymptotic expressions for the free energy (12):

$$G_{EDL}^{lamella} = kTN_{surf}\left(-\ln\left(vc_{ref}e^2W_0\right) + \frac{\pi^2}{4\left(\tilde{W}+1\right)} + o\left(\frac{1}{\tilde{W}^3}\right)\right), \quad \tilde{W}\to\infty, \tag{13}$$

$$G_{EDL}^{lamella} = kTN_{surf}\left(-\ln\left(vc_{ref}e^2W_0\right) + \ln\left(\frac{1}{3}+\frac{1}{\tilde{W}}\right) + 1 + o\left(\tilde{W}\right)\right), \ \tilde{W}\to 0 \tag{14}$$

By differentiating the asymptotic expression (13) with respect to the distance between the monolayers $2r_0$, one can obtain the well-known Langmuir equation for the disjoining pressure [33]:

$$P = 2\varepsilon\varepsilon_0(\pi kT/q)^2/(2r_0)^2 \tag{15}$$

For the cylindrical reverse micelle, we have an explicit expression

$$G_{EDL}^{cylinder} = kTN_{surf}\left(-\ln\left(vc_{ref}e^2W_0\right) + \ln\left(1+\frac{1}{\tilde{W}}\right) + \frac{1}{\tilde{W}}\ln\left(1+\tilde{W}\right)\right) \tag{16}$$

For spherical reverse micelles, we have a numerical solution and the following approximate formula:

$$\frac{G_{EDL}^{sphere}}{kTN_{surf}} + \ln\left(vc_{ref}e^2W_0\right) \approx \ln\left(1+\frac{1.48371699}{\tilde{W}}\right) + \frac{4}{3\tilde{W}}\ln\left(1+0.45408719\tilde{W}\right), \tag{17}$$

whose maximum absolute and relative errors are 0.016 at $\tilde{W}=1$ and 0.015 at $\tilde{W}=3$, respectively. Equation (17) is asymptotically exact at $\tilde{W}\to 0$ and at $\tilde{W}\to\infty$.

Note that the term $\ln(vc_{ref}e^2W_0)$ in Eqs. (12), (16), and (17) is just a constant, which does not affect the differences in free energies between different shapes of reverse micelles.

Comparison of the free energies for different shapes

Figure 2 shows the calculated free energies of the EDL in reverse micelles of different shapes. We see that the free energy increases in the order lamella<cylinder<sphere. That is, lamellar reverse micelles are the most favorable. It is also seen that for lamellar reverse micelles, contrary to the Helfrich equation, the dependence of the EDL free energy on the molar ratio W is quite strong. This dependence may be considered as a volume contribution, as discussed in the "Introduction."

Qualitatively, the dependency of the EDL free energy on the molar ratio W may be interpreted as a result of the tendency of counterions to be dissolved in a large volume of water. The free energy difference between the reverse micelles of different shapes is mainly due to the difference in the curvature of the surfactant monolayer. At the same molar ratio, the curvature increases in the order lamella<cylinder<sphere. The higher the curvature, the lower the volume effectively available for the counterions concentrated near the surface.

To analyze the contribution of the curvature to the EDL free energy, we have subtracted the free energy for lamellar reverse micelles from the free energies for spherical and cylindrical reverse micelles. It turned out that the free energy differences are approximately proportional to each other. For $\tilde{W}$ larger than approximately 2, their ratio is almost equal to 4/3. This value is in accordance with that obtained from the first-order Taylor expansion of the free energy in powers of the principal curvatures:

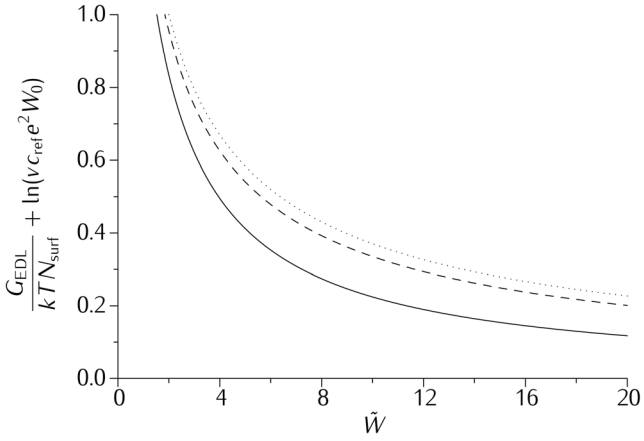

Fig. 2 The calculated free energies of the EDL for the lamellar (*solid line*), cylindrical (*dashed line*), and spherical (*dotted line*) reverse micelles. For AOT reverse micelles, the range $0<\tilde{W}<20$ corresponds to the range $0<W<60$

$$\sigma(c_1, c_2) = \sigma(0,0) + \frac{\partial\sigma(0,0)}{\partial c_1}(c_1 + c_2) \tag{18}$$

Indeed, using Eqs. (4) and (18), we obtain for the ratio of the curvature-dependent parts of the free energies of spherical and cylindrical reverse micelles

$$\frac{G_{EDL}^{sphere} - G_{EDL}^{lamella}}{G_{EDL}^{cylinder} - G_{EDL}^{lamella}} = \frac{\frac{1}{r_{sphere}} + \frac{1}{r_{sphere}}}{\frac{1}{r_{cylinder}} + \frac{1}{\infty}} = 2\frac{r_{cylinder}}{r_{sphere}} = 2\frac{2vW/a_0}{3vW/a_0} = \frac{4}{3} \tag{19}$$

Equation (19) also follows from Eqs. (16) and (17) in the limit $\tilde{W}\to\infty$. Hence, one can decompose with reasonable accuracy the EDL free energy into the volume and surface parts. However, although Eq. (19) holds, the concept of the curvature dependence of the free energy is not fully applicable for the surface part of the EDL free energy because, according to Eqs. (16) and (17), the coefficient of c_1+c_2 in Eq. (18) is not constant but increases with $\tilde{W}$:

$$\frac{\partial\sigma(0,0)}{\partial c_1} = \frac{kT}{\pi\lambda_B}\left(\ln\left(\tilde{W}+3\right) + 1 - \frac{\pi^2}{4} + O\left(\frac{1}{\tilde{W}}\right)\right), \quad \tilde{W}\to\infty, \tag{20}$$

where $\lambda_B = q^2/(4\pi\varepsilon\varepsilon_0 kT)$ is the Bjerrum length (7 Å for monovalent ions in water at 298.15 K). A similar conclusion that the bending energy parameters vary with the water-to-surfactant molar ratio has been reached in the studies [22, 27–29] by considering the undulating membranes in charged lamellar phases. This result holds for the case of no added salt (counterions only). There are also studies [20, 21, 25, 26] in which the rigidity constants of charged membranes and monolayers are calculated in the limit of high added salt concentration and, therefore, do not vary with the water content.

Qualitative mechanism of the thermodynamic preference for the spherical shape of reverse micelles

As discussed in the "Introduction," the curvature dependence of the free energy, taken alone, cannot explain why spherical reverse micelles can be stable over a wide range of water-to-surfactant molar ratios. Also, it cannot be explained by taking into account only the EDL free energy. But, taking into account both contributions, we can understand the sphericity. To show this, let us first consider the EDL contribution to the free energy (Fig. 2). As discussed above, the EDL free energy can be approximately decomposed into the volume and surface parts. By definition, the volume part is the same for all shapes. But the surface part depends on the shape of reverse micelles because their mean curvatures are different. Therefore, the surface part governs the equilibrium shape. For the surface part of the EDL free energy, the coefficient of c_1+c_2 in Eq. (18) is positive, whereby the lamellar reverse micelles are most favorable: they have the lowest free energy curve (Fig. 2). To make the spherical reverse micelles the most favorable, it is necessary to modify the free energy by adding a term that changes the sign of the surface part. The most obvious candidate for this term is the intrinsic curvature dependence of the free energy of the surfactant monolayer. Let us take this intrinsic curvature dependence in the simplest form of Eq. (18) with the coefficient of c_1+c_2 equal to $-k_0$, where $k_0>0$. Then, k_0 may be adjusted in such a way that the addition of the curvature dependence (18) to the EDL free energy may invert the order of the curves in Fig. 2 and thus make the spherical shape the most favorable. In this case, the intrinsic curvature dependence overcomes the curvature dependence associated with the EDL. However, the EDL curvature dependence is characterized by the variable coefficient (20), which increases with $\tilde{W}$. Hence, for any fixed k_0, there always exists a number $\tilde{W}_0$ such that for $\tilde{W}>\tilde{W}_0$, the intrinsic curvature dependence cannot overcome that of the EDL and the lamella remains the most favorable shape. Thus, for sufficiently large k_0, we have the spheres for $\tilde{W}<\tilde{W}_0$ and the lamellas for $\tilde{W}>\tilde{W}_0$. In a more rigorous consideration, the transition between spheres and lamellas is not sharp; there is a region of coexistence of different shapes, whose quantities are determined by the common tangent to the free energy curves.

A more accurate model of AOT reverse micelle

For the sake of clarity, the above calculations were performed using a highly simplified model of the reverse micelle. We now make two adjustments to the model.

First, we must take into account that the negative charges of the dissociated surfactant molecules are not located exactly at the surface of the water core but are deepened to some extent. This causes the surface charge density to depend on the radius of the reverse micelle. Moreover, the EDL becomes bilateral: the counterions are distributed both inside and outside the surface of the negative charges. For AOT reverse micelles, the negative charges are immersed in the water core to a depth of 2.3 Å. This value has been calculated from the results of the molecular dynamics simulation carried out by Nevidimov et al. [35, 36]. The negative charges of the dissociated AOT molecule are located primarily on the sulfonate group. It is the size of the sulfonate group that determines the depth of immersion.

Second, we must obtain an accurate equation for the dependence of the water core radius on the water-to-surfactant molar ratio W. Experiments show that this dependence is linear [37, 38]. It is usually [39, 40] interpreted in terms of the equation

$$r_0 = \frac{nv}{a_0} W + \frac{nv_H}{a_0}, \tag{21}$$

where v_H is volume of the water-immersed portion of the surfactant, n=3 (for spheres). For v_H=0, Eq. (21) reduces to Eq. (4). For AOT reverse micelles, the analysis of experimental data with Eq. (21) gives the following: v_H=222 Å^3, a_0= 63 Å^2 [40]. However, the seemingly obvious interpretation of the linear dependence of the water core radius on the molar ratio W in terms of Eq. (21) is not quite correct. The problem is that for a curved interface, the area a_0 per one surfactant molecule depends on the position of the mathematical surface used to define this area. In fact, Eq. (21) assumes that this surface coincides with the boundary of the water core. But, there are no grounds for this assumption. To define a_0, it is more correct to use the surface of inextension, introduced in the "Introduction." The area per one surfactant molecule at this surface does not depend on the size of the reverse micelle. The equation for the radius of the surface of inextension is analogous to Eq. (21):

$$r_{inext} = \frac{nv}{a_0} W + \frac{n(v_{H1} + v_{H2})}{a_0}, \tag{22}$$

where v_{H1} is the true volume of the water-immersed portion of the surfactant molecule and v_{H2} is the volume of the portion of the surfactant molecule between the surface of inextention and the boundary of the water core. The distance between the surface of inextension and the boundary of the water core is approximately v_{H2}/a_0. By subtracting this distance from the radius of the surface of inextension (22), we obtain for the radius of the water core

$$r_0 = \frac{nv}{a_0} W + \frac{nv_{H1} + (n-1)v_{H2}}{a_0} \tag{23}$$

Hence, the volume v_H, determined from the experimental data using Eq. (21), is not, in fact, the volume of the hydrophilic portion of the surfactant molecule, but the sum $v_{H1}+(n-1)/n$ v_{H2}. For AOT reverse micelles, this sum is, as noted above, 222 Å^3. In order to find the terms of this sum separately, let us estimate the first term v_{H1} in an independent manner. For this purpose, we note that the water-immersed portion of the AOT molecule consists of the sulfonate group and the counterion. It follows from the results of the molecular dynamics simulation mentioned above and is supported by the solubility considerations (see Online Resource). The volume of the water-immersed portion of the AOT molecule may be estimated to be 62 Å^3 from the close-packing considerations using the known density and molar mass of sodium dithionate dihydrate: $(SO_3Na)_2$ $2H_2O$, 242 g/mole, 2.19 g/cm^3 [41]. Now, the quantity v_{H2} in Eq. (23) can be estimated as (222–62)×3/(3–1) Å^3= 240 Å^3. Then, it follows that the surface of inextension is located at the distance v_{H2}/a_0=3.8 Å from the boundary of the water core.

The noncoincidence of the surface of inextention and the boundary of the water core leads to the dependence of the area of the water core per one surfactant molecule on the size of the reverse micelle. Therefore, the expression for the free energy must contain a term that takes into account the interfacial tension at the boundary of the water core γ_{core}:

$$G_{total} = G_{EDL} + \gamma_{core} A_\Omega, \tag{24}$$

where G_{total} is the total free energy of the reverse micelle, A_Ω is the area of the boundary of the water core Ω. It is the second term on the right-hand side of Eq. (24) that leads to the intrinsic curvature dependence discussed in the previous section.

Now, we have a model accurate enough to describe AOT reverse microemulsions. In this model, the force balance in the surfactant shell of the reverse micelle can be qualitatively understood by considering two adjacent surfactant molecules as two rods pivotally connected at the point of contact on the surface of inextension. The angle between these rods depends on the size of the reverse micelle. These rods are acted upon by attractive forces due to the interfacial tension and by the repulsive forces due to the EDL. The total moment of these forces about the point of contact gives rise to the curvature dependence of the free energy. In this model, the interfacial tension is the only driving force that causes reverse micelles to be spherical because, for given W, among all the shapes under consideration, the sphere has the highest curvature and, consequently, the smallest area of the interface per one surfactant molecule.

Besides the interfacial tension and the EDL, there are some other factors that may affect the free energy: for example, the curvature dependence of the packing of the surfactant tails [18, 42], the interfacial tension at the outer boundary of the

reverse micelle, the free energy of mixing of reverse micelles with the solvent. We do not take these factors into account, considering them to be negligible (see Online Resource).

Preliminary calculations using the refined model of reverse micelle

Calculation of the most favorable shape

The equations given above for the EDL were modified to take into account that the negative charges of the surfactant molecules are immersed in the water core.

To perform the numerical calculations, we have all the necessary parameters except the interfacial tension γ_{core}, which is therefore a free parameter that must be adjusted to fit the experimental data. The range of its possible values can be estimated from the observation that the fragments of the surfactant molecule just above the surface of the water core are structurally similar to the molecules of methyl acetate or ethyl acetate. The interfacial tension of the water–ethyl acetate interface is 6.8 mJ/m^2, and that of the water–alkane interface is 50 mJ/m^2 [43]. The interfacial tension at the surface of the water core must lie between these two values. Calculations with different values of γ_{core} shows that the value corresponding to a reasonably wide range of stability of spherical reverse micelles (approximately up to $W=50$) is approximately 22 mJ/m^2. For this value, the free energies of reverse micelles of different shapes are compared in Fig. 3. The figure shows that the most favorable shape is the sphere at low W and the lamella at high W. For other values of the interfacial tension, the behavior of the free energy of reverse micelles can be found in Online Resource.

Thus, the model predicts the transition to lamellar reverse micelles at high water-to-surfactant molar ratios. It should be noted that the flat geometry of lamellar reverse micelles allows a large contact area between them. Therefore, they can attract each other so strongly that they settle out as a separate phase that can no longer be called "reverse microemulsion." Thus, if the calculations predict that the lamella is an optimal shape of reverse micelles, then it should be interpreted as a formation of the corresponding new phase. The sphere-to-lamella transition has been experimentally observed earlier for reverse microemulsions based on carefully purified AOT [44–46]. It should also be noted that for a poor nonpolar solvent, as W increases, the intermicellar interactions may cause phase separation into two reverse microemulsions with different droplet concentrations before the transition to lamellar reverse micelles can occur [47].

The situation is different for AOT containing impurities: a two-phase system of the type "reverse microemulsion+water" may be formed at intermediate water-to-surfactant molar ratios [44]. The most significant impurities contained in commercial AOT are the AOT hydrolysis products and inorganic salts remaining after the synthesis [44, 48]. We now proceed to calculate the lowest-free-energy state of a reverse microemulsion system with salt impurities.

Calculations for reverse microemulsions with salt impurities

The free energy of the "oil+water+surfactant+salt" system was minimized with respect to the shape of reverse micelles, the amount of the separate water phase, and the amount of salt remaining in the reverse micelles after the separation (the salt concentration in the separated water may be considerably higher than in the solubilized water [49–51]). As an example, Fig. 4 shows the result of the calculation for the case of AOT contaminated by sodium sulfate at a molar ratio of 1:400. We see that in the presence of an impurity, a two-phase system of the type "reverse microemulsion+water" may be formed at intermediate values of W. In this calculation, the ratio of the spatially averaged salt concentration in the water core to the salt concentration in the separated water varies from about 8 to about 14. Such high ratios are expected when the amount of the separated water is small compared to the amount of solubilized water [50], which is the case here.

The amount of separated water and the boundaries of the two-phase region depend on the amount of impurity. At low impurity-to-AOT molar ratio (in our case, less than 1:650), the water is completely solubilized.

These results are in qualitative agreement with the corresponding experimental data obtained by Kunieda et al. [44]. In both cases, there is a transition to lamellar structures at high water contents; when the surfactant contains salt impurities, a water phase separates from the reverse microemulsion at intermediate values of W; the effect of salt impurities is very strong.

Testing the model: thermodynamic calculations

Chemical potentials and polydispersity

The model developed above can be used to calculate various thermodynamic properties of AOT reverse microemulsions. We start with the calculation of the chemical potentials of water and surfactant:

$$\mu_w = \left(\frac{\partial G}{\partial N_w}\right)_{N_{surf}} = f'(W), \quad \mu_{surf} = \left(\frac{\partial G}{\partial N_{surf}}\right)_{N_w} = f(W) - W f'(W), \tag{25}$$

where N_w is the number of water molecules in the reverse micelle, $G=N_{surf} f(W)$ is the free energy of reverse micelles. The values of $f(W)$ can be taken from Fig. 3. The result is shown in Fig. 5. The chemical potential of water increases

with increasing W, tending to the bulk value, which we arbitrarily set to zero. The surfactant chemical potential is a decreasing function of W. In the coexistence region, the chemical potentials do not depend on W.

In principle, the calculated chemical potential of water can be checked experimentally by measuring the relative humidity above the microemulsion at equilibrium. However, since at $W>10$, the relative humidity varies very slowly with W, the accuracy of the measurements in this interval must be very high. Meanwhile, at $W<10$, most of the water is bound, and therefore, our model itself cannot be quantitatively accurate. At $W=10$, the calculated chemical potential of water is $-0.01kT$, which corresponds to a relative humidity of 0.99. Literature experimental values for the relative humidity over AOT reverse microemulsions at $W=10$ range from 0.89 to 0.98 [52–54].

The results for the chemical potential of water (Fig. 5) can be used to calculate the relative standard deviation (ε_w) of the water-to-surfactant molar ratio (w) of an individual reverse micelle (see Eq. 42 of [40]). If we neglect the shape fluctuations of reverse micelles and recall that their size is approximately proportional to W, then ε_w becomes approximately equal to their polydispersity. The polydispersity thus obtained ranges from 27 % for $W=3$ to 10 % for $W=60$. These values do not contradict the experimental data, which, however, show considerable scatter [40].

Enthalpy

Let us calculate the enthalpy of water solubilization by the solution of AOT in oil:

$$\Delta H_{\text{total}} = H_{\text{total}}(W) - H_{\text{total}}(0), \tag{26}$$

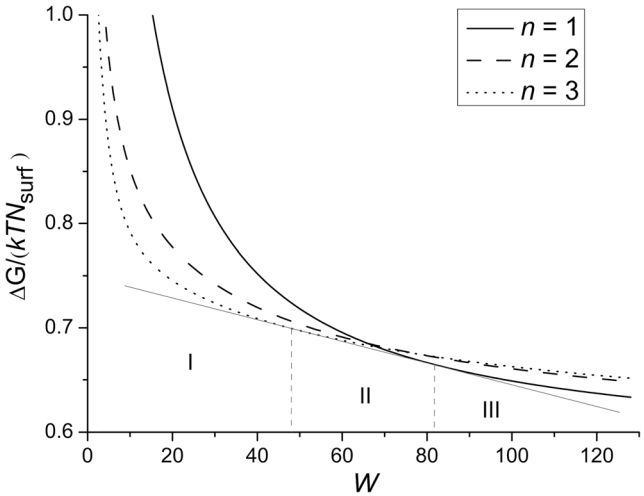

Fig. 3 Free energies of reverse micelles of different shapes at $\gamma_{\text{core}}=22$ mJ/m^2. Spherical reverse micelles are stable at $W<48$ (*region I*); lamellar, at $W>83$ (*region III*). At intermediate values of W, there is a coexistence of spheres and lamellas (*region II*). The coexistence region is determined by the common tangent to the free energy curves. $T=298.15$ K

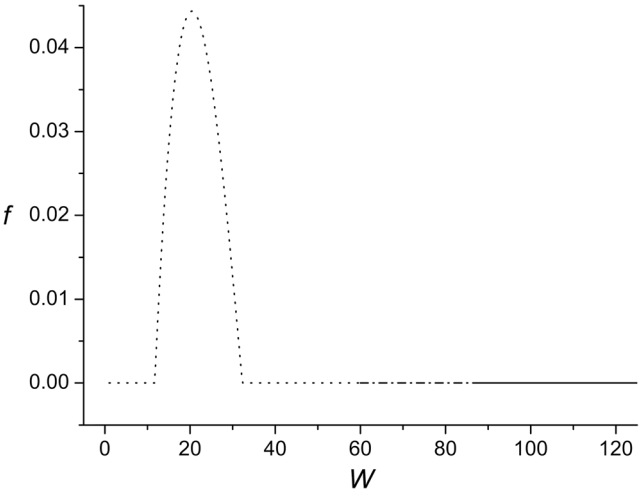

Fig. 4 Calculated fraction of the separated water f for the case of AOT contaminated by sodium sulfate at a molar ratio of 1:400. In the range $12<W<32$, a two-phase system is formed ($f>0$). The *dotted line* shows the region of spherical reverse micelles ($W<60$); the *solid line* corresponds to lamellas ($W>88$); the *dash-dotted line* means the region of coexistence of spheres and lamellas ($60<W<88$). $T=298.15$ K

where $H_{\text{total}}(W)$ is the enthalpy of the system as a function of W. This function can be obtained from G_{total} by using the Gibbs–Helmholtz equation. The temperature derivative of G_{total} appears in this equation. It can be obtained by numerical differentiation, which requires calculations at different temperatures. Therefore, we must take into account that some parameters in our model may be temperature dependent. In fact, there are two such parameters. The first parameter is the dielectric constant of water ε. Its temperature dependence can be found in [41]. The second parameter is the interfacial tension γ_{core}. As a rough estimate, it can be assumed that γ_{core} is determined primarily by the contacts between the water and the alkane portions of the AOT molecules. Then, the temperature dependence of γ_{core} is the same as that for the interfacial tension between water and n-alkane. For the latter (from hexane to dodecane), the temperature dependence [55, 56] in the range 278.15–323.15 K may be expressed as

$$\frac{T}{\gamma}\frac{d\gamma}{dT} = -0.52 \pm 0.02 \tag{27}$$

The results of the calculations, together with the literature experimental data [57, 58], are shown in Fig. 6. We see that the calculated and measured enthalpies are in semiquantitative agreement. The small deviation may be due to incomplete dissociation of the surfactant molecules. The figure also shows the results of calculations for $\gamma_{\text{core}}=0$. Comparing the curves, we see that the enthalpy of solubilization is determined mainly by the interfacial tension at the boundary of the water core.

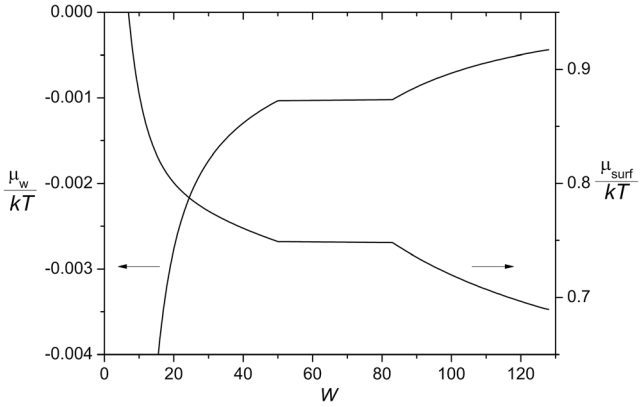

Fig. 5 Chemical potentials of water and surfactant versus *W*

Phase diagram

In Section 5, we have calculated the most favorable state of the reverse microemulsion system at a fixed temperature of 298.15 K. By repeating these calculations for different temperatures, we can obtain the phase diagram in the *W*–*T* plain. As far as we know, calculations on the *W*–*T* phase diagrams of AOT reverse microemulsion systems have never been performed before.

The result for the case of AOT contaminated by sodium sulfate at a molar ratio of 1:400 is shown in Fig. 7. The calculated phase diagram is in qualitative agreement with those observed experimentally [44, 47, 59, 60]. The lowest curve in Fig. 7 encloses the region IV, where the reverse microemulsion coexists with an excess water phase. This curve is known as a solubilization curve [59]. The curve between regions I and II is referred to as a solubility curve [59]. Above this curve, the solubility of reverse micelles in the nonpolar solvent is not sufficient to prevent their aggregation, caused, in our model, by the formation of lamellar reverse micelles. For the explanation of the hyperbolic shape of the solubility curve, see Online Resource.

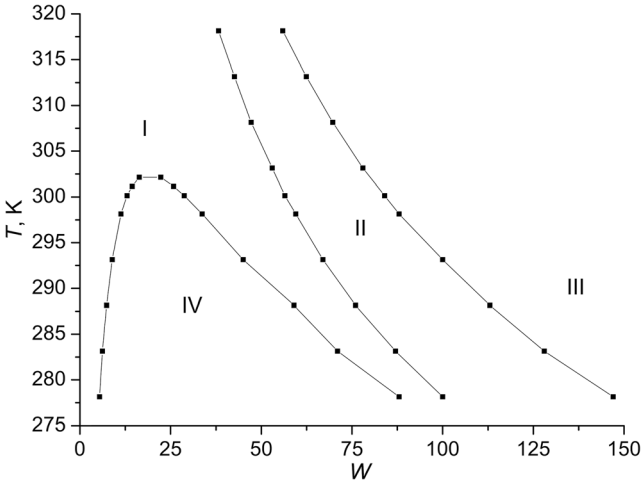

Fig. 7 Phase diagram of the reverse microemulsion system based on AOT contaminated by sodium sulfate at a molar ratio of 1:400. *Roman numerals* denote the following regions. *I.* The one-phase region with spherical reverse micelles. *II.* The region of coexistence of spherical and lamellar reverse micelles (in reality, lamellar reverse micelles must aggregate and form a separate phase). *III.* The region of lamellar reverse micelles. *IV.* The two-phase region (reverse microemulsion+water)

The *W*–*T* phase diagram of the reverse microemulsion system based on pure AOT is shown in Fig. 8. The region of spherical reverse micelles (I) widens slowly with decreasing the temperature down to 277 K and then shrinks abruptly. The discontinuity results from the fact that with decreasing temperature, the curvature dependence increases and eventually overcomes the disjoining pressure, thereby blocking the solubilization. As this takes place, the common tangent to the *W*-dependencies of the free energies of spherical and lamellar reverse micelles suddenly changes one of the points of tangency at a certain temperature (at this temperature, the tangent touches one of the free energy curves at two points simultaneously).

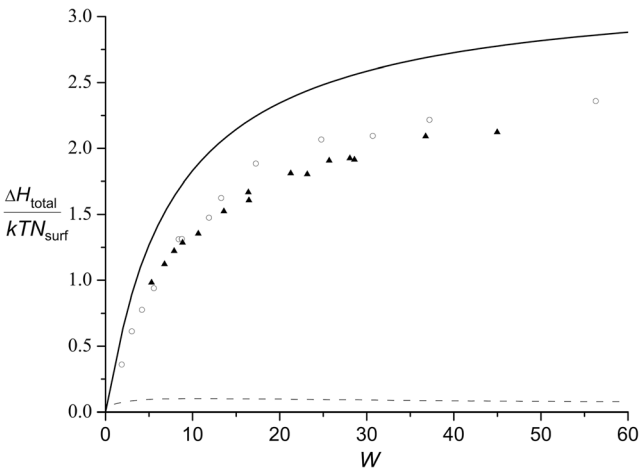

Fig. 6 Enthalpy of water solubilization versus *W* at 298.15 K. *Solid line*: calculation. *Open circles*: experimental data from [57]. *Solid triangles*: experimental data from [58]. *Dashed line*: calculation for $\gamma_{core}=0$

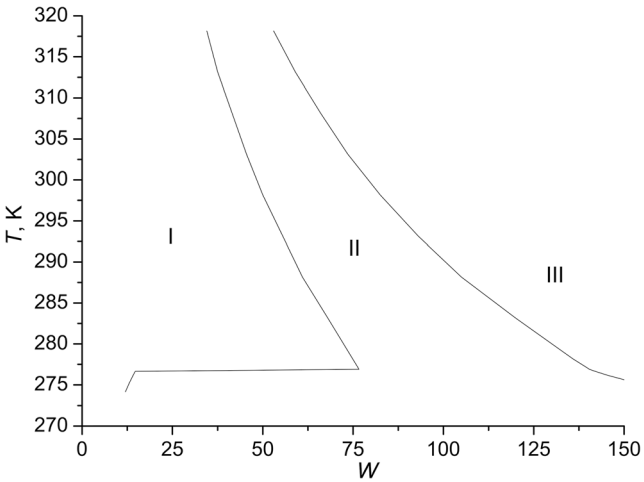

Fig. 8 Phase diagram of the reverse microemulsion system based on pure AOT. *Roman numerals* denote the same regions as in Fig. 7

Previously, this effect has been observed experimentally for reverse microemulsion systems formulated with carefully purified AOT [44].

Conclusions

In this paper, we have shown that in order to understand why AOT reverse microemulsion droplets can be spherical over a wide range of water-to-surfactant molar ratios, it is necessary to take into account both the disjoining pressure and the bending energy. The latter can be taken in its simplest form (the first-order Taylor expansion in the principal curvatures). To check this, we have carried out the free-energy calculations for AOT-based reverse microemulsions. For these microemulsions, the disjoining pressure results from the electrical double layer; the bending energy results from the interfacial tension at the boundary of the water core and the noncoincidence of this boundary with the surface of inextention. The accuracy of the results obtained in this way is sufficient for an approximate calculation of the thermodynamic and structural properties of AOT reverse microemulsion systems: the most favorable shape of reverse micelles, the chemical potentials of water and surfactant, the polydispersity, the enthalpy of water solubilization, and the phase diagram (in particular, in the presence of salt impurities).

For reverse microemulsions based on ionic surfactants with monovalent counterions, the electrical double-layer contribution to the free energy is of prime importance and, at the same time, cannot be adequately represented by the Helfrich equation, which is widely used to describe reverse microemulsions, including that of AOT.

Although the detailed calculations have been carried out here only for reverse microemulsions based on AOT, the main idea of the paper is expected to be valid for any surfactant: if reverse micelles are spherical over a wide range of water-to-surfactant molar ratios, then there must be a repulsive disjoining pressure in the water core. For some surfactants, such as ionic surfactants with monovalent counterions, the presence of significant disjoining pressure is an established fact. For other surfactants, e.g., zwitterionic, the disjoining pressure is expected to be low. Therefore, by considering whether the disjoining pressure exists for a given surfactant, it is possible to draw some conclusions about the structure of microemulsion.

Finally, we note that all calculations in this paper were performed assuming complete dissociation of the surfactant molecules. Since this assumption has led to results consistent with experimental data, it can be accepted as a first approximation. Moreover, it is clear from the Langmuir equation (15) that the disjoining pressure does not depend on the surface charge density and, hence, on the degree of dissociation. However, since the counterion concentration near the surface of the water core is high, dissociation may be incomplete and may depend on the size of reverse micelles. Therefore, further progress in improving the accuracy of calculations requires quantitative data on the degree of dissociation.

Acknowledgments This work was supported by the Russian Foundation for Basic Research (Grant Nos. 12-03-31496 and 13-03-00681).

References

1. Ivanchikhina AV, Tovstun SA, Razumov VF (2013) Influence of surfactant polydispersity on the structure of polyoxyethylene (5) nonylphenyl ether/cyclohexane/water reverse microemulsions. J Colloid Interface Sci 395:127–134
2. Wennerström H (1996) Thermodynamic theory of surfactant phases. Curr Opin Colloid Interface Sci 1:370–375
3. Strey R (1996) Phase behavior and interfacial curvature in water-oil-surfactant systems. Curr Opin Colloid Interface Sci 1:402–410
4. Hellweg T (2002) Phase structures of microemulsions. Curr Opin Colloid Interface Sci 7:50–56
5. Gradzielski M (2008) Recent developments in the characterisation of microemulsions. Curr Opin Colloid Interface Sci 13:263–269
6. Sjöblom J, Lindberg R, Friberg SE (1996) Microemulsions—phase equilibria characterization, structures, applications and chemical reactions. Adv Colloid Interface Sci 65:125–287
7. Helfrich W (1973) Elastic properties of lipid bilayers: theory and possible experiments. Z Naturforsch C J Biosci 28:693–703
8. Sicoli F, Langevin D, Lee LT (1993) Surfactant film bending elasticity in microemulsions: structure and droplet polydispersity. J Chem Phys 99:4759–4765
9. Borkovec M, Eicke HF, Ricka J (1989) Polydispersity in dilute microemulsions: a consequence of the monomer-droplet equilibrium. J Colloid Interface Sci 131:366–381
10. Borkovec M (1989) From micelles to microemulsion droplets: size distributions, shape fluctuations, and interfacial tensions. J Chem Phys 91:6268–6281
11. Eriksson JC, Ljunggren S (1990) The multiple chemical equilibrium approach to the theory of droplet microemulsions. Prog Colloid Polym Sci 81:41–53
12. Eriksson JC, Ljunggren S (1995) Thermodynamic evaluation of the polydispersity of droplet microemulsions. Langmuir 11:1145–1153
13. Eriksson JC, Ljunggren S, Kegel WK, Lekkerkerker HNW (2001) Entropy and droplet size distributions of winsor I and II microemulsions. Colloids Surf A 183:347–360
14. Arleth L, Pedersen JS (2001) Droplet polydispersity and shape fluctuations in AOT [bis(2-ethylhexyl)sulfosuccinate sodium salt] microemulsions studied by contrast variation small-angle neutron scattering. Phys Rev E 63:061406 (18 pages)
15. Kitchens CL, Bossev DP, Roberts CB (2006) Solvent effects on AOT reverse micelles in liquid and compressed alkanes investigated by neutron spin-echo spectroscopy. J Phys Chem B 110:20392–20400
16. Kegel WK, Bodnar I, Lekkerkerker HNW (1995) Bending elastic moduli of the surfactant film and properties of a winsor II microemulsion system. J Phys Chem 99:3272–3281
17. Borkovec M (1992) Phenomenological theories of globular microemulsions. Adv Colloid Interface Sci 37:195–217
18. Szleifer I, Kramer D, Ben-Shaul A, Gelbart WM, Safran SA (1990) Molecular theory of curvature elasticity in surfactant films. J Chem Phys 92:6800–6817
19. Fogden A, Hyde ST, Lundberg G (1991) Bending energy of surfactant films. J Chem Soc Faraday Trans 87:949–955

20. Lekkerkerker HNW (1990) The electric contribution to the curvature elastic moduli of charged fluid interfaces. Physica A 167:384–394
21. Duplantier B, Goldstein RE, Romero-Rochín V, Pesci AI (1990) Geometrical and topological aspects of electric double layers near curved surfaces. Phys Rev Lett 65:508–511
22. Daicic J, Fogden A, Carlsson I, Wennerström H, Jönsson B (1996) Bending of ionic surfactant monolayers. Phys Rev E 54:3984–3998
23. Ennis J (1992) Spontaneous curvature of surfactant films. J Chem Phys 97:663–678
24. Fogden A, Mitchell DJ, Ninham BW (1990) Undulations of charged membranes. Langmuir 6:159–162
25. Winterhalter M, Helfrich W (1988) Effect of surface charge on the curvature elasticity of membranes. J Phys Chem 92:6865–6867
26. Mitchell DJ, Ninham BW (1989) Curvature elasticity of charged membranes. Langmuir 5:1121–1123
27. Higgs PG, Joanny JF (1990) Enhanced membrane rigidity in charged lamellar phases. J Phys Fr 51:2307–2320
28. Harden JL, Marques C, Joanny JF, Andelman D (1992) Membrane curvature elasticity in weakly charged lamellar phases. Langmuir 8: 1170–1175
29. Fogden A, Daicic J, Mitchell DJ, Ninham BW (1996) Electrostatic rigidity of charged membranes in systems without added salt. Physica A 234:167–188
30. Linse P, Gunnarsson G, Jönsson B (1982) Electrostatic interactions in micellar solutions. a comparison between Monte Carlo simulations and solutions of the Poisson–Boltzmann equation. J Phys Chem 86: 413–421
31. Guldrand L, Jönsson B, Wennerström H, Linse P (1984) Electrical double layer forces. A Monte Carlo study J Chem Phys 80:2221–2228
32. Wennerström H, Khan A, Lindman B (1991) Ionic surfactants with divalent counterions. Adv Colloid Interface Sci 34:433–449
33. Israelachvili JN (1998) Intermolecular and surface forces. Academic Press
34. Jönsson B, Wennerström H (1981) Thermodynamics of ionic amphiphile–water systems. J Colloid Interface Sci 80:482–496
35. Nevidimov AV, Razumov VF (2009) Molecular dynamics simulations of AOT reverse micelles' self-assembly. Mol Phys 107:2169–2180
36. Nevidimov AV, Razumov VF (2013) Molecular dynamics simulation of reverse micelles: a search for the most efficient strategy. Colloid J 75:191–219
37. Kotlarchyk M, Chen SH, Huang JS (1982) Temperature dependence of size and polydispersity in a three-component microemulsion by small-angle neutron scattering. J Phys Chem 86:3273–3276
38. Amararene A, Gindre M, Le Huérou JY, Urbach W, Valdez D, Waks M (2000) Adiabatic compressibility of AOT [sodium bis(2-ethylhexyl)sulfosuccinate] reverse micelles: analysis of a simple model based on micellar size and volumetric measurements. Phys Rev E 61:682–689
39. Nave S, Eastoe J, Heenan RK, Steytler D, Grillo I (2000) What is so special about aerosol-OT? 2. Microemulsion Syst Langmuir 16: 8741–8748
40. Tovstun SA, Razumov VF (2010) On the composition fluctuations of reverse micelles. J Colloid Interface Sci 351:485–492
41. CRC Handbook of Chemistry and Physics (2003–2004) ed. by D.R. Lide, 84th ed.
42. Szleifer I, Ben-Shaul A, Gelbart WM (1990) Chain packing statistics and thermodynamics of amphiphile monolayers. J Phys Chem 94: 5081–5089
43. Donahue DJ, Bartell FE (1952) The boundary tension at water-organic liquid interfaces. J Phys Chem 56:480–484
44. Kunieda H, Shinoda K (1979) Solution behavior of aerosol OT/water/oil system. J Colloid Interface Sci 70:577–583
45. Tamamushi B, Watanabe N (1980) The formation of molecular aggregation structures in ternary system: aerosol OT/water/iso-octane. Colloid Polym Sci 258:174–178
46. Hall AC, Tekle E, Schelly ZA (1989) Flow birefringence in the L2 phase of the aerosol OT/isooctane/water system. Langmuir 5:1263–1265
47. Fletcher PDI, Howe AM, Robinson BH (1987) The kinetics of solubilisate exchange between water droplets of a water-in-oil microemulsion. J Chem Soc Faraday Trans 1(83):985–1006
48. Sager WFC (1998) Systematic study on the influence of impurities on the phase behavior of sodium bis(2-ethylhexyl) sulfosuccinate microemulsions. Langmuir 14:6385–6395
49. Biais J, Barthe M, Bourrel M, Clin B, Lalanne P (1986) Salt partitioning in winsor type II systems. J Colloid Interface Sci 109: 576–585
50. Van Aken GA, Overbeek JTG, De Bruijn PL, Lekkerkerker HNW (1993) Partitioning of salt in winsor II microemulsion systems with an anionic surfactant and the consequences for the phase behavior. J Colloid Interface Sci 157:235–243
51. Van Nieuwkoop J, Snoei G (1985) Phase diagrams and composition analyses in the system sodium dodecyl sulfate/butanol/water/sodium chloride/heptane. J Colloid Interface Sci 103:400–416
52. Ueda M, Schelly ZA (1988) Mean aggregation number and water vapor pressure of AOT reverse micellar systems determined by controlled partial pressure–vapor pressure osmometry (CPP-VPO). Langmuir 4:653–655
53. Chew CH, Wong MK (1991) Relative water vapor pressure of water-in-oil microemulsions by headspace gas chromatographic analysis. J Dispers Sci Technol 21:495–501
54. Kubik R, Eicke HF (1982) On the activity of water and the concept of the interfacial free energy in W/O-microemulsions. Helv Chim Acta 65:170–177
55. Aveyard R, Haydon DA (1965) Thermodynamic properties of aliphatic hydrocarbon/water interfaces. Trans Faraday Soc 61:2255–2261
56. Zeppieri S, Rodríguez J, López de Ramos AL (2001) Interfacial tension of alkane+water systems. J Chem Eng Data 46:1086–1088
57. Rouviere J, Couret JM, Lindheimer A, Lindheimer M, Brun B (1976) Structure des agrégats inverses d'AOT. II. Effets de sel sur les micelles inverses. J Chim Phys Phys Chim Biol 76:297–301
58. D'Aprano A, Lizzio A, Turco Liveri V (1987) Enthalpies of solution and volumes of water in reversed AOT micelles. J Phys Chem 91: 4749–4751
59. Kon-No K, Kitahara A (1971) Solubility behavior of water in non-aqueous solutions of Oil-soluble surfactants: effect of molecular structure of surfactants and solvents. J Colloid Interface Sci 37: 469–475
60. Kon-No K, Kitahara A (1972) Secondary solubilization of electrolytes by di-(2-ethylhexyl) sodium sulfosuccinate in cyclohexane solutions. J Colloid Interface Sci 41:47–51